Received: 12 May 2019 | Revised: 9 August 2019 | Accepted: 30 August 2019

DOI: 10.1002/dac.4214

RESEARCH ARTICLE

WILEY

Analyzing lifetime of energy harvesting underwater wireless sensor nodes

H. Emre Erdem | **V. Cagri Gungor**

Computer Engineering Department, Abdullah Gul University, Turkey

Correspondence
H. Emre Erdem, Department of Computer Engineering, Abdullah Gul University, Kayseri, 38060, Turkey.
Email: huseyin.erdem@agu.edu.tr

Funding information
Turkish Scientific and Technical Research Council (TUBITAK), Grant/Award Number: 114E248

Summary

Underwater Wireless Sensor Networks (UWSNs) are utilized to monitor underwater environments that pose many challenges to researchers. One of the key complications of UWSNs is the difficulty of changing node batteries after their energy is depleted. This study aims to diminish the issues related to battery replacement by improving node lifetime. For this goal, three energy harvesting devices (turbine harvester, piezoelectric harvester, and hydrophone harvester) are analyzed to quantitate their impacts on node lifetime. In addition, two different power management schemes (schedule-driven and event-driven power management schemes) are combined with energy harvesters for further lifetime improvement. Performance evaluations via simulations show that energy harvesting methods joined by power management schemes can improve node lifetime substantially when actual conditions of Istanbul Bosporus Strait are considered. In this respect, turbine harvester makes the biggest impact and provides lifetime beyond 2000 days for most cases, while piezoelectric harvester can perform the same only for low duty cycle or event arrival values at short transmission ranges.

KEYWORDS
energy harvesting, node lifetime, power management, underwater wireless sensor networks

1 | INTRODUCTION

Over two-thirds of the Earth's surface is covered with water in the form of oceans, seas, rivers, and lakes. Underwater world created as a result of these formations is rich in natural resources (eg, oil and valuable minerals) and is largely unexplored. Recently, there has been an increasing demand from both industry and academia for the development and deployment of Underwater Wireless Sensor Networks (UWSNs) to better exploit underwater environments. The envisioned industrial, scientific, environmental, commercial, and military applications span a very wide range, including pipeline monitoring, seismic monitoring, environmental pollution monitoring, tactical surveillance, natural resource detection, and assisted navigation.[1,2] In such UWSN applications, nodes in the network are responsible for performing measurement of environmental variables and send their data to a sink node for further analysis and decision making.

In UWSNs, acoustics communication is usually preferred over radio frequency or optical communication mainly due to its significantly greater transmission ranges. However, increased path loss, propagation delay, and error rates of acoustics channel cause power consumption of transceiver hardware to be much higher than that of terrestrial networks.[3] Such high consumption renders existing battery technology insufficient in energizing network nodes for extended durations. In underwater applications, replacing batteries is not considered as a viable solution since accessing

deep waters is a costly and challenging task.[4] As a result, either additional technologies that will supply more energy to the nodes should be integrated or power consumption of underwater nodes should be decreased.

Energy harvesting methods that exploit ambient energy to generate electrical energy has been a notable solution to improve node lifetime. This way, the outputs of harvester devices are used to support batteries powering underwater nodes. There exist different energy harvester devices exploiting different resources, such as mechanical, electromagnetic, or thermal ambient energy. Analyzing the outputs of different harvesters is vital to prove their effectiveness on lifetime extension.

In addition to increasing available energy, decreasing node power consumption is also helpful for extended lifetime. Decreased power consumption can be achieved by adopting less power-hungry hardware or better power management scheme. While the impact of the former is limited by existing hardware technology, the latter may decrease the node's power consumption via algorithms that disable certain hardware components when they are not in use. Power management schemes also enable providing results for application scenarios with different measurement requirements. In this respect, while some applications require periodic measurements, others need measurements upon an event arrival, which alters energy consumption characteristics significantly.

This study aims to analyze how much energy harvesting devices can extend underwater node lifetime when used with different power management schemes. The application scenario focuses on a single node that transmits its packets of measurement data to a sink node. The main contributions of this paper are listed as follows:

- Impact of energy harvesting on node lifetime is analyzed when different power management methods are adopted. To better evaluate the impact, realistic communication channel model and environmental parameters are utilized.
- The impact of energy harvesting is calculated for three different harvester types (hydrokinetic turbine, acoustic hydrophone, and piezoelectric cantilever) to cover a wider range of possible implementations.
- Two different power management schemes (schedule-driven and event-driven power management schemes) are utilized to consider application specific priorities. To this end, schedule-driven schemes put emphasis on periodic measurements, while event-driven schemes require an event occurrence to perform measurements.

The paper is organized as follows: Section 2 informs the reader about various underwater energy harvesting research conducted to this date. Section 3 provides an overview of the simulated environment and explains the energy harvesting methods, power management schemes, and channel model used in this study. Section 4 presents the simulation results followed by Section 5 concluding the paper.

2 | RELATED WORK

In literature, there exists numerous research to improve underwater node or network lifetime using energy harvesting devices. Hydrokinetic energy is among the most prominent resource for underwater energy harvesting. Hydrokinetic turbines are commonly used to exploit hydrokinetic energy to generate electricity. Authors of [5] use turbines at deep waters and solar panels on shallow waters to supply power to sensor nodes. In addition, the proposed HyDRO algorithm considers residual energy levels to decrease average power consumption of the network. Results with varying inter packet arrival times depict significant positive impact of the algorithm on network lifetime.

In another study utilizing turbines, generated power output is increased by providing mobility instead of fixing turbines in place.[6] Attaching turbines on an underwater vehicle enables exploiting underwater flows with higher degree of freedom resulting in higher efficiency.

Turbine harvester is also adopted in [7] to support node batteries combining with a sleep mechanism. In study, nodes send their measurement to a sink node at around 140 m of distance. However, the results do not include a lifetime analysis explaining the impact of harvesting or sleep cycles.

Piezoelectric material, which generates electricity when exposed to mechanical stress, is another commonly used medium to convert hydrokinetic energy into electrical energy by attaching them to beam structures.[8] These structures that are forced to perform perpetual forward-backward movement exert push-pull forces on the piezoelectric material causing electricity generation. In a study adopting piezoelectric cantilever, laminar flow of water is disturbed with a cylindrical object perpendicular to the direction of flow.[9] The disturbed flow causes mechanical stress on coupled piezoelectric cantilever initiating electricity generation. In this study, Molino-Minero-Re et al manage to generate up to 0.31 μW of power in water flow of only 0.1 m/s.

In another study, Shahab et al create piezoelectric beam with macro-fiber composite structure to analyze the amount of generated electrical energy for different beam sizes.[10] Their work analyzes and compares air and water flow scenarios. According to results, power density in underwater scenario is much higher than that of air flow case.

Toma et al propose a novel hardware design that utilizes piezoelectric bimorphs to exploit mechanical movement of water particles to generate electrical energy via a pendulum-like structure.[11] Their work is capable of providing sufficient power to a network with nodes utilizing high sleep rates.

Authors in [12] use piezoelectric-based energy harvesting to energize body implanted underwater transmitters that are used for animal monitoring. The implant helps generate the required power through fishs natural movements. Although transmission range in their experiments was quite short, the study represents the first on-body implementation of its kind.

Similar to piezoelectric materials, ionic polymer metal composite (IPMC) materials also generate electricity when bent. A unique study conducted by Cha et al uses IPMC shaped as an annular plate.[13] The movement of the base at the center of the plate generates vibration on the plate itself, which creates a voltage difference between the two electrodes of IPMC.

Ambient energy in underwater environments can also be found in chemical form. Rezaei et al create a galvanic cell using river water as electrolyte.[14] They manage to harvest 25 μW of power, which is sufficient for continuously energizing some low-power Wireless Sensor Network nodes with low transceiver power requirement.

Biomass is another resource for electricity generation in underwater environments. Wang et al uses microbial fuel cells to exploit underwater biomass to generate electricity to power sensor nodes.[15] Their study is capable of improving lifetime harvesting energy between measurements. Also in [16] microbial fuel cells enable continuous monitoring with around 96% event detection rate.

Acoustic noise is recently started to be used as a resource for underwater harvesters. Bereketli and Bilgen propose a novel method to remotely power sensor nodes using hydrophones.[17] The study consists of an acoustic source connected to power grid and remotely positioned multiple sensor nodes. The acoustic signal emitted from the source is used to generate electricity on the nodes using a hydrophone array. This way, the nodes are able to operate continuously with low duty cycles using 1 kW of power at the acoustic source.

All the abovementioned research work provide valuable efforts for energy harvesting in underwater environments using various energy sources and hardware as listed in Table 1. However, while some of them disregard the impact of underwater acoustic propagation characteristics, others simply omit how power management schemes or adopting different types of it may impact lifetime. In our previous study, this gap is partially filled considering hydrokinetic turbine and hydrophone harvester as well as two power management schemes.[18] The objective of this paper is to carry the study further by adding piezoelectric harvester and considering different transmission distances. This way, the impacts of energy harvesting and underwater propagation characteristics on underwater node lifetime are analytically quantified. Also, using power management schemes, lifetime for different application requirements are analyzed.

3 | PROPOSED SOLUTION

This section provides detailed information on calculations for generated and consumed power levels. While generated power levels are affected by harvester outputs, consumed power levels are mainly affected by power management

TABLE 1 Underwater energy harvesting research

Based on	Hardware
Solar and mechanical energy [5]	Solar panel and turbine
Mechanical energy[6,7]	Turbine
Mechanical energy[8-12]	Piezoelectric beam
Mechanical energy[13]	IPMC
Chemical energy[14]	Galvanic cell
Biomass[15,16]	Microbial fuel cell
Acoustic energy[17]	Hydrophone

Abbreviation: IPMC, ionic polymer metal composite.

schemes and acoustics communication channel conditions. The following subsections provide insights into energy harvesting methods, power management methods, and acoustics communication channel after providing a general overview of the simulated environment.

A. System overview

Throughout this study, an underwater intrusion detection scenario, where a node is responsible for monitoring underwater environment, is adopted. As default, the node is equipped with a color camera that generates the data to be transmitted using an acoustic modem. Since this study focuses on node lifetime, calculations focus on a single communication link between the node and a sink node on the water surface as depicted in Figure 1. The location of the sink on horizontal plane changes based on the transmission range of node. In simulations, the node performs measurements and transmits its data directly to the sink node. Timing of measurements and subsequent transmissions is decided by a power management scheme. The network is assumed to be using carrier sense multiple access (CSMA) as its medium access control (MAC) protocol. Since there is no relay node between the transmitter and the sink node, there is no advanced routing layer consideration.

Throughout the study, an underwater sensor node is assumed to have 4 hardware units, namely, communication, processing, sensing, and power, as shown in Figure 2. In the figure, the items with an asterisk represent additional hardware used when event driven power management is preferred.

In a node, communication unit performs all transmission/reception tasks required for the node to talk to the sink node. Processing unit is responsible for reading sensors and generating data packets. Sensing unit represents sensors that convert environmental parameters into electrical signal, which is used both for data generation and event detection. Finally, power unit supplies required power to other units at any time and charges the batteries using harvested energy. The states of the hardware units with active power consumption are provided in Section 3.3.

B. Energy harvesting methods

Using energy harvesting methods to extend node lifetime can decrease battery replacement requirements significantly. Existing harvesting devices can generate electrical energy exploiting ambient energy available in mechanical, thermal, and electromagnetic forms.[19,20] In this study, energy is harvested using hydrokinetic turbine, piezoelectric cantilever, or

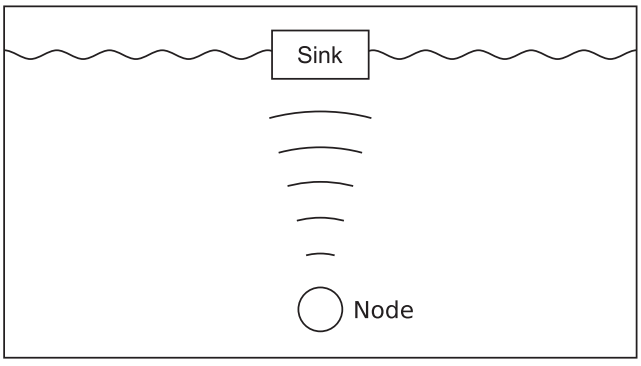

FIGURE 1 System overview

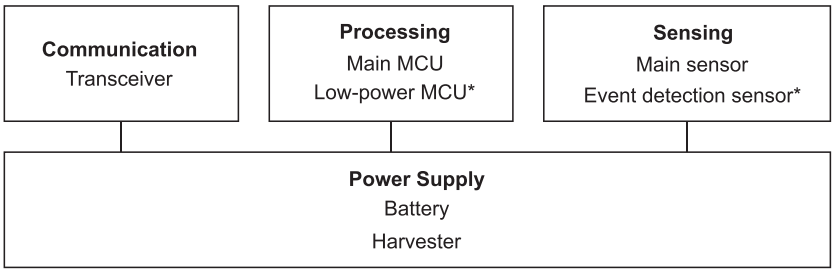

FIGURE 2 Node hardware

hydrophone. The output of these harvesters is assumed to be continuously used for charging battery. The magnitudes of the harvested power levels are calculated based on the previous research conducted in these areas under the conditions of a specific environment.

1. Hydrokinetic turbine

Hydrokinetic turbines illustrated in Figure 3 convert kinetic energy of the water current into electrical energy. Since the planned location of application, Istanbul Bosporus Strait, provides water crossing between Black Sea and Sea of Marmara, it provides a highly suitable environment for hydrokinetic turbine usage as harvester. The flow rates of Bosporus Strait are given in Table 2.[21]

As seen in the Table 2, the flow rate almost stops at the depth of 13 m. This is the result of Bosporus Strait having two layers of flow within its maximum depth of 55 m. The upper layer flows from Black Sea to Sea of Marmara and the lower layer flows in the opposite direction. This situation is explicit in average flow rate values as well.

Output power calculation for hydrokinetic turbine is similar to that of previous studies.[22,23] The harvesting device explained in this section is a horizontal axis hydrokinetic turbine with a rotor radius of 5 cm. The power that a water current flowing through the wing spanning area possesses can be calculated as follows:

$$P = \frac{1}{2}\rho A \vartheta^3 \tag{1}$$

In Equation (1), ρ, A, and υ represent water density, circular wing-spanning area, and flow rate, respectively. However, the turbine cannot exploit all the energy water current possesses. In this study, the value of 0.06 is used as the harvesting efficiency coefficient.

2. Piezoelectric cantilever

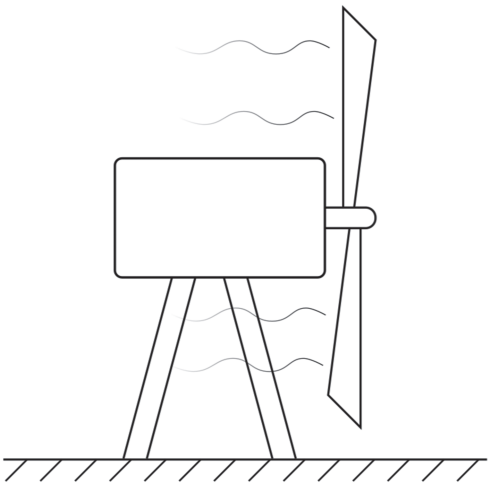

FIGURE 3 Hydrokinetic turbine

TABLE 2 Water flow rates for Istanbul Bosporus Strait[21]

Depth(m)	Min. (m/s)	Max. (m/s)	Avg. (m/s)	Std. dev. (m/s)
6.3	−2.32	1.18	−0.91	0.74
10.3	−2.18	1.20	−0.42	0.61
13.3	−1.72	1.20	−0.03	0.45
20.3	−0.38	1.06	0.55	0.16
40.3	0.42	1.14	0.65	0.08

In addition to turbines, eel-like flexible beam structures with piezoelectric material are also used to scavenge the energy of water currents. This type of harvesting devices exploit vertical movement of the cantilever beam with piezoelectric material positioned parallel to the flow as shown in Figure 4. Bending of the beam structure asserts physical stress on the piezoelectric material, which results in power generation. The external force that causes bending is created via a bluff, which disturbs the smooth flow of water stream. The behavior of the disturbed currents is explained via Kármán vortex street.[24]

To calculate the power output of the piezoelectric cantilever, the equations presented in [25] are adopted. The formula for maximum generated power from a single piezoelectric harvester is

$$P = 2f(W_{el\_cw} + W_{el\_ccw}) \tag{2}$$

where f, $W_{el\text{-}cw}$, and $W_{el\text{-}ccw}$ represent vortex frequency and electrical energy in clockwise and counterclockwise directions. The frequency and electrical energy is calculated using Equations (3) and (4).

$$f = \frac{Sr \times \vartheta}{D} \tag{3}$$

$$W_{el} = \frac{1}{128} p^2 \frac{{d_{31}}^2 BL^5}{\varepsilon_0 \varepsilon_r {T_{pzt}}^3} \tag{4}$$

In [3], Sr and D represent Strouhal number and bluff size. D is calculated dividing the cantilever length by 2.125 to enable the beam oscillate only with its first harmonic mode[24]. In Equation (4), p, d_{31}, B, ε_0, ε_r, L, and T_{pzt} represent pressure difference, piezoelectric constant, beam width, absolute permittivity, relative permittivity, cantilever length, and cantilever thickness, respectively. To calculate the electrical energy for different directions pressure difference, Equations (5) and (6) are used.

$$p_{cw} = \frac{\rho}{2}\vartheta^2 \tag{5}$$

$$p_{ccw} = -\frac{3}{2}\rho\vartheta^2 \tag{6}$$

3. Hydrophone

Another resource for harvesting in underwater environment is the ambient acoustic noise. Hydrophones can be used to generate electrical energy from acoustic sound waves. In this respect, the sufficiency of the noise generated by ships passing through the Strait for harvesting is analyzed.

This study assumes using five hydrophones in array as shown in Figure 5. The amount of power each hydrophone supply is calculated using[17]

$$P = \frac{\frac{RL + RVS}{10}^{10}}{4R_p} \tag{7}$$

FIGURE 4 Piezoelectric cantilever

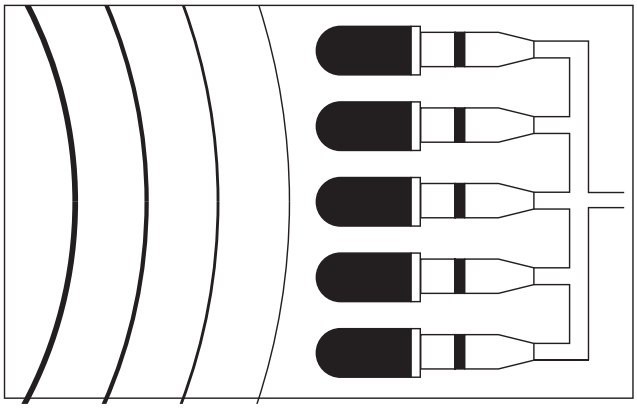

FIGURE 5 Hydrophone array

In Equation (7), *RL* is received level in dB, *RVS* is the receiving voltage sensitivity of the hydrophone in dB, and R_p is the impedance of the hydrophone. In simulations, HTI-90-U hydrophone from High-Tech Inc. is used.[26] This hydrophone provides an RVS value of −186 dB re 1 V/μPa without preamplifier. For impedance, 125 Ω is the preferred value.

To calculate *RL*, attenuation level formula is used with Source Level (*SL*) values for container ships from [27].

$$RL = SL - AL \tag{8}$$

where,

$$AL = 20 \times \log_{10} d + \alpha(f) \times d \tag{9}$$

In Equation (9), $\alpha(f)$ represents frequency dependent attenuation coefficient and calculation of this parameter is explained in Section 3.4.

The power formula in Equation (7) provides the entire available acoustic power. However, the hydrophone cannot exploit the entire available energy. Thus, an efficiency coefficient of 0.7 is selected.

The total energy a ship provides throughout its single pass is calculated using

$$E_{ship} = \int_{t=0}^{\frac{l_{max}}{v}} P(t)dt \tag{10}$$

where l_{max} is the maximum horizontal distance between the ship and the mote and is taken 400 m as harvested energy levels drastically decrease beyond this range. Figure 6 depicts this distance for a typical ship passage scenario.

The *d* parameter shown in Figure 6 that represents the direct distance between the ship and the mote is calculated using

$$d = \sqrt{\left(\frac{l_{max}}{2}\right)^2 + depth^2} \tag{11}$$

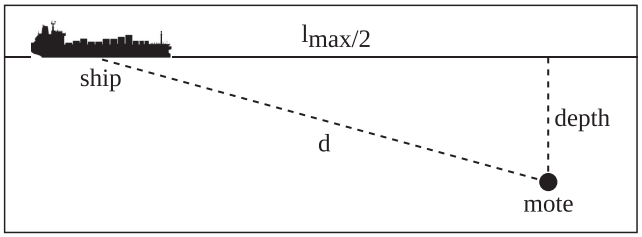

FIGURE 6 Distance parameters for hydrophone

The average power that can be harvested from all the ships (n_{ship}) that pass through the strait in a day is calculated via

$$P_{daily_{avg}} = \frac{E_{ship} \times n_{ship}}{24 \times 60 \times 60} \tag{12}$$

The harvested power values calculated using the above formulas are subtracted from the power consumption values to calculate the net power consumption.

$$P_{net\_cons} = P_{cons} - P_{harv} \tag{13}$$

C. Power management methods

Although energy harvesting methods may provide significant amount of energy, they still need to be combined with efficient power management methods to further extend lifetime. Consideration of power management schemes with different duty cycle and event arrival values enable evaluating distinct application scenarios.

In this study, schedule-driven and event-driven power management schemes as implemented in [28] are used.

1. Schedule-driven scheme

In schedule-driven scheme, each node is turned on and off with predefined intervals. Using such switching mechanism makes distinguishable contribution to node lifetime based on duty cycle value. The state transition diagram for schedule-driven operation that depicts the tasks within each cycle as semi-Markov chain is shown in Figure 7. This scheme comprises four states, namely, sleep, monitoring, processing, and communication. β parameter in the diagram represents the probability of event detection, therefore fourth state is divided into two substates representing the same state with different event presence. α parameter shows successful data transmission probability. Also, processing and communication tasks are activated only when an event is detected.

The hardware statuses for all the states can be seen in Table 3.

Using such separated states eases lifetime calculation. The lifetime of a node in terms of cycles is calculated via

$$Lifetime = \frac{E_{total}}{P_{per\_cycle}} \tag{14}$$

where, P_{per_cycle} represents the power usage in a single cycle consisting above-mentioned states. The formula used to

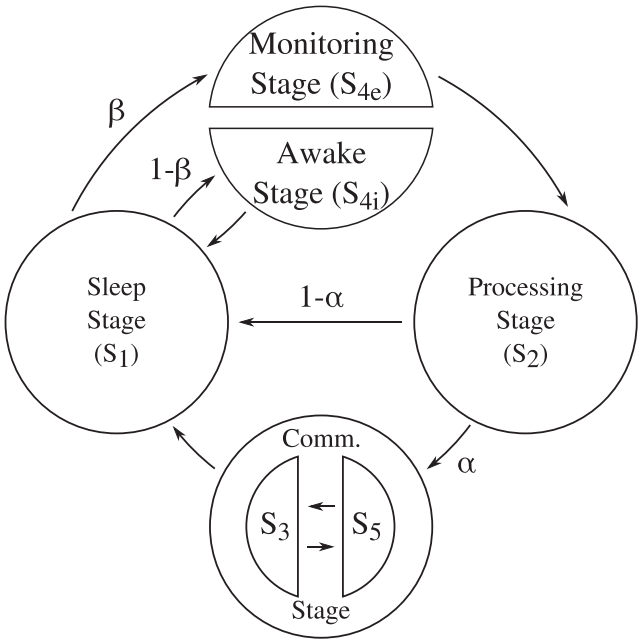

FIGURE 7 State transition diagram for schedule-driven operation

TABLE 3 Hardware status for schedule-driven operation[28]

State	Radio	CPU	Sensor
S_1	OFF	OFF	OFF
S_2	OFF	ON	ON
S_3	TX	ON	OFF
S_4	OFF	IDLE	ON
S_5	RX	ON	OFF

calculate this value considering the possibility of an event detection is shown in Equation (15).

$$P_{per_{cycle}} = \frac{P_e + \frac{\beta}{T_c} E_e}{1 + \frac{\beta}{T_c}} T_e \tag{15}$$

In Equation (15), P_e is the average power consumption of sleep and monitoring states including CPU wake-up energy consumption, T_c is the entire period duration, T_e is the extra time spent for event detection, and E_e is the extra energy used for event detection.

Although this scheme is effective in decreasing power consumption, increased chance of missed events during sleep is not desired in sensitive applications such as warfare intrusion detection.

2. Event-driven scheme

Schedule-driven scheme is not preferable in applications intolerant to missed events since it cannot provide extended lifetime without risking event detection. For such applications, event-driven scheme offers a better solution.

In event-driven scheme, each node has additional sensor and processor for sensing and processing tasks besides regular hardware. Although this complementary hardware uses much less power compared to regular hardware, it is only used for event detection since it cannot measure the actual data. Waking the actual processor and sensor only after an event detection, power consumption is substantially decreased. In this study, the sensor and microcontroller used for event detection are BII-7070 series directional hydrophone with BII-1060 low power low noise hydrophone preamplifier

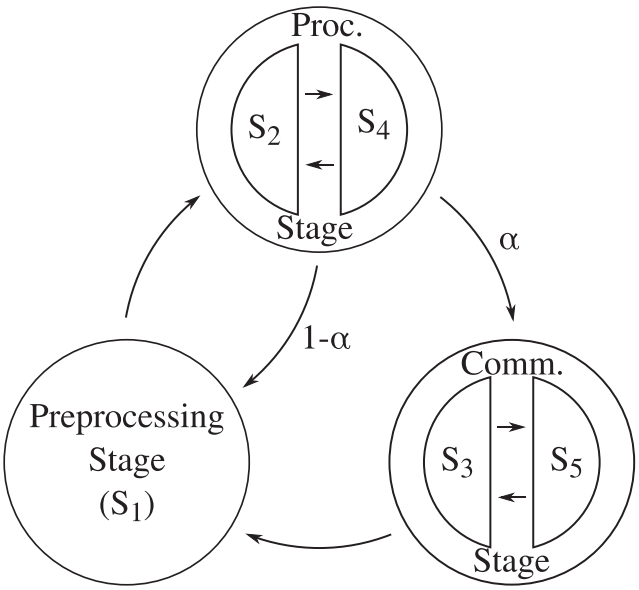

FIGURE 8 State diagram for event-driven operation

TABLE 4 Hardware status for event-driven operation[28]

State	Preprocessor	Radio	CPU	Sensor
S_1	ON	OFF	OFF	OFF
S_2	ON	OFF	ON	ON
S_3	ON	TX	ON	OFF
S_4	ON	OFF	IDLE	ON
S_5	ON	RX	ON	OFF

and Microchip PIC10F200 microcontroller.[29,30] As opposed to harvesting via hydrophone case, the sensing hardware requires power supply due to preamplifier usage. In case of event detection, the central CPU with color camera is activated. The state transition diagram of event-driven scheme can be seen in Figure 8. As opposed to the former scheme, event-driven scheme has low-power (preprocessing) state instead of sleeping state.

α parameter in the diagram represents the probability of the detected event to be sent to the sink node. Also, hardware statuses can be seen in Table 4. Preprocessor column represents both low power CPU and sensor.

The power consumption per cycle is calculated using Equation (16).

$$P_{per\_cycle} = \frac{P_m + \lambda E_e}{1 + \lambda T_e} \tag{16}$$

In Equation (16), P_m and λ represent the energy spent for monitoring and event arrival rate, respectively.

D. Acoustics communication channel model

A review of recent literature shows that employing acoustic signals has usually been the first choice for practical implementations of UWSNs due to their extended communication ranges compared with radio frequency and optical signals.[3,31] Using underwater acoustic channel, the main issue affecting node lifetime is high-energy requirements of radio hardware due to excessive attenuation levels and error rate of the channel. Importantly, in underwater acoustic channel conditions, path loss depends on signal frequency and the distance between the communicating nodes. In this study, the channel model presented in [32] is adopted. However, in places where the transmission power value calculated using the model is smaller than that specified in the datasheet of the acoustic modem, the values listed in the datasheet are used.[33]

According to this model, source level at certain distance and frequency, *SL(d,f),* in dB with 0 directivity index can be modeled as

$$SL(d,\ f) = A(d,\ f) + N(f) + SNR \tag{17}$$

where, *A(d,f)* and *N(f)* represent path loss and ambient noise values. *SNR* value is the signal to noise ratio at the receiver node. According to this model, path loss is calculated using

$$A(d,\ f) = \kappa \log(d) + \alpha(f) d 10^{-3} \tag{18}$$

In Equation (18), κ value represents spreading factor. Practical spreading ($\kappa = 15$) is the preferred spreading type. In addition, *α(f)* represents frequency dependent absorption coefficient, and it is found using Equation (19).

$$\alpha(f) = \gamma_1 \frac{f_1 f^2}{f_1 + f^2} + \gamma_2 \frac{f_2 f^2}{f_2 + f^2} + \gamma_3 f^2 \tag{19}$$

where,

$$f_1 = 0.78 \left(\frac{S}{35}\right)^{\frac{1}{2}} e^{\frac{T}{26}} \tag{20}$$

$$f_2 = 42e^{\frac{T}{17}} \tag{21}$$

$$\gamma_1 = 0.106e^{\frac{pH-8}{0.56}} \tag{22}$$

$$\gamma_2 = 0.52\left(1+\frac{T}{43}\right)\left(\frac{S}{35}\right)e^{\frac{-h}{6}} \tag{23}$$

$$\gamma_3 = 0.00049e^{-\left(\frac{T}{27}+\frac{h}{17}\right)} \tag{24}$$

In above equations, T represents temperature in °C, pH represents water acidity, and S represents water salinity.

The total ambient noise in Equation (17) is the sum of water turbulence, surface ship, thermal noise, and breaking waves ambient noise as shown in Equation (25).

$$N(f) = N_t(f) + N_s(f) + N_{th}(f) + N_w(f) \tag{25}$$

The components of ambient noise are calculated using

$$10\log(N_t(f)) = 17 - 30\log(\mathrm{f}) \tag{26}$$

$$10\log(N_s(f)) = 40 + 20(s-0.5) + 26\log(\mathrm{f}) - 60\log(f+0.03) \tag{27}$$

$$10\log(N_{th}(f)) = -15 + 20\log(f) \tag{28}$$

$$10\log(N_w(f)) = 50 + 7.5w^{\frac{1}{2}} + 20\log(f) - 40\log(f+0.4) \tag{29}$$

In Equations (26) to (29), s and w represent shipping and wind factor, which are assumed 0.5 and 1, respectively. To calculate the *SL*, *SNR* should be computed first. This is performed via

$$SNR = 10^{\frac{SNR(d,f)}{10}} \tag{30}$$

$$SNR(d,\ f) = \frac{E_b\ R}{N_0 B_N} \tag{31}$$

To calculate *SNR* using Equation (31), SNR per bit value (E_b/N_0), data rate value (R), and noise bandwidth (B_N) value should be used. SNR per bit value can be calculated using Equation (32) since *BER* value for the sensor mote is known.

$$BER = \frac{3}{8}erfc\left(\sqrt{\frac{4\ E_b}{10N_0}}\right) \tag{32}$$

After the source level is found using Equation (17), transmission power can be calculated using the intensity at 1 m of distance, I_t.

$$I_t = \frac{P_{tx}}{2\pi \times 1m \times h} \tag{33}$$

$$SL(d,\ f) = 10\log\left(\frac{I_t}{I_0}\right) \tag{34}$$

In Equations (33) and (34), h and I_0 represent the water depth and reference intensity of $0.67\text{x}10^{-18}$.

TABLE 5 Simulation parameters for turbine harvester

Parameter	Value	Unit
Blade radius	0.05	m
Turbine Efficiency	0.06 [23]	-
Flow rate (υ)	0.65 [21]	m/s

TABLE 6 Simulation parameters for piezoelectric harvester

Parameter	Value	Unit
Relative permittivity (ε_r)	504[34]	-
Length (L)	40	Mm
Width (B)	3	Mm
Thickness (T_{pzt})	60	μm
Piezoelectric constant (d_{31})	$750\text{x}10^{-12}$ [35]	C/N
Strouhal number (Sr)	0.2[36]	-

TABLE 7 Simulation parameters for hydrophone harvester

Parameter	Value	Unit
Receiving voltage sensitivity (RVS)	−186[26]	dB re 1 V/μPa
Hydrophone impedance (R_p)	125[17]	Ω
Noise at source level (SL)	188.1[27]	dB
Daily ship passages (n_{ship})	2000	-

TABLE 8 Simulation parameters for acoustic channel

Parameter	Value	Unit
Temperature (T)	15	°C
Acidity (pH)	8	-
Salinity (s)	35	g/kg
Data rate (R)	2000	bps
Noise bandwidth (B_N)	1000	Hz
Packet size	140	Byte

TABLE 9 Harvested power levels

Harvester type	Value	Unit
Turbine harvester	64.41	mW
Piezoelectric harvester	8.57	mW
Hydrophone harvester	0.03	mW

4 | PERFORMANCE RESULTS

The results presented in this section are gathered using MATSNL toolbox on MATLAB.[28] For all the harvesting scenarios, the node is assumed to be positioned at 40.3 m of depth, where it is closest to the sea bottom, where flow rate information is available. Total energy available in the batteries is 5.175 Wh. Also, BER value of 1e-10 is used as specified by the acoustic modem datasheet.[33] This way, the channel model is used to calculate the required transmission power to satisfy this BER value. Tables 5–8 provide parameters used for harvesters.

Harvested average power levels for each device are presented in Table 9. It is evident that turbine harvester performs significantly better in scavenging. Moreover, the average harvested power by hydrophone is quite low compared with other devices. However, it should be noted that the sizes of the harvesters are not the same and, altering the dimensions, power outputs may be improved. Also, the preferred environment and depth favors the turbine and piezoelectric harvester. Choosing a shallower depth, the performance of hydrophone harvester can be improved.

Figures 9–16 show lifetime results for different power management schemes and transmission distances. Figures 9–12 use schedule-driven power management with transmission ranges of 200 m, 400 m, 800 m, and 1600 m. Similarly, Figures 13–16 use event-driven scheme with the same transmission ranges. Compared with varying event arrival values on event-driven operation, schedule-driven operation uses a fixed value of 1000 event arrivals per day and varying duty cycle values. In each figure, lifetime values with different combinations of harvesters and power management schemes

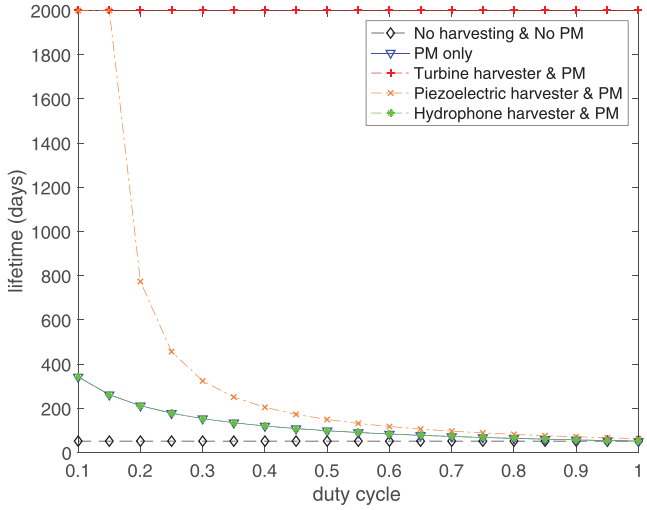

FIGURE 9 Lifetime improvement with schedule-driven operation at 200 m transmission range

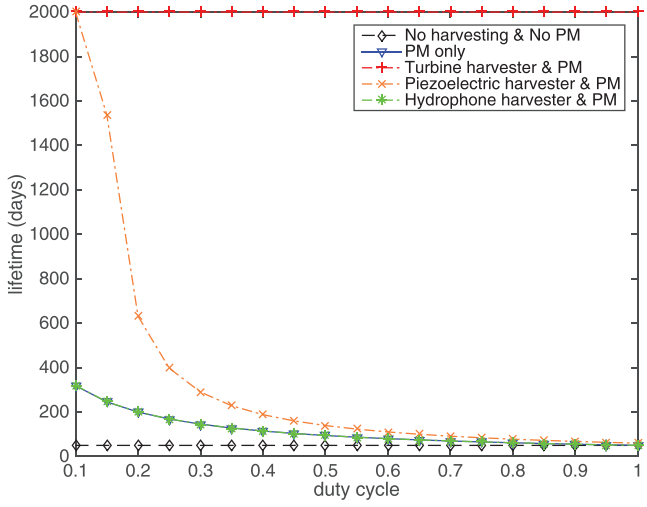

FIGURE 10 Lifetime improvement with schedule-driven operation at 400 m transmission range

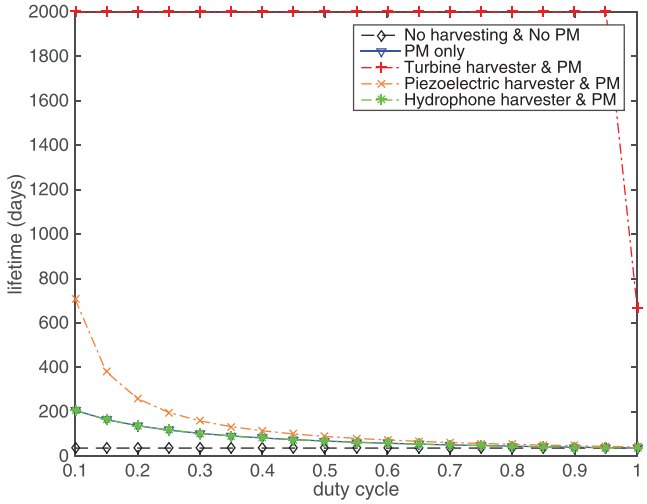

FIGURE 11 Lifetime improvement with schedule-driven operation at 800 m transmission range

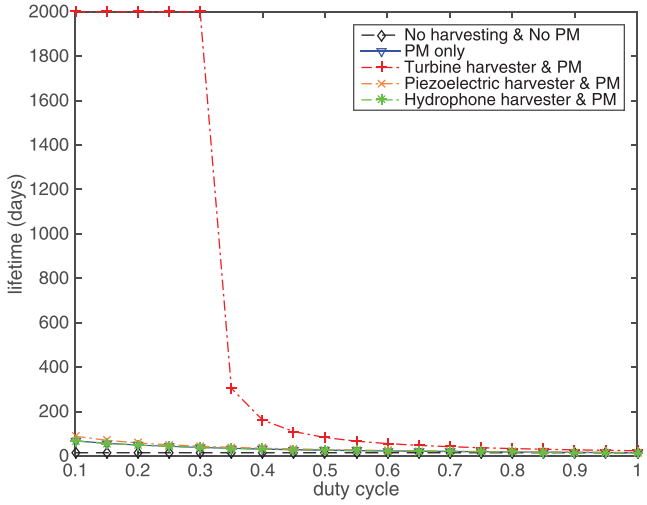

FIGURE 12 Lifetime improvement with schedule-driven operation at 1600 m transmission range

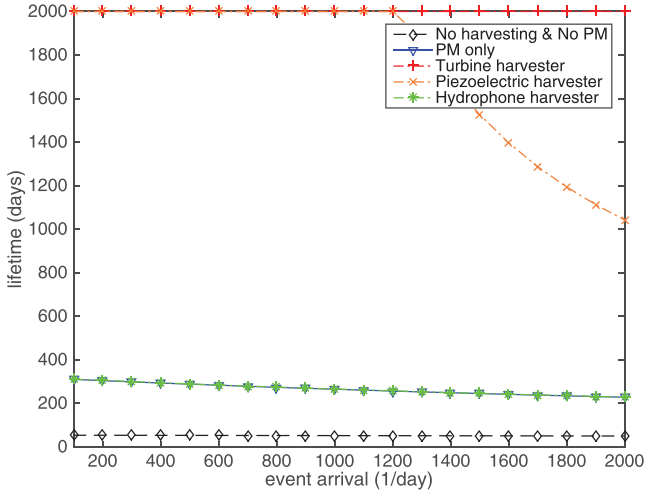

FIGURE 13 Lifetime improvement with event-driven operation at 200 m transmission range

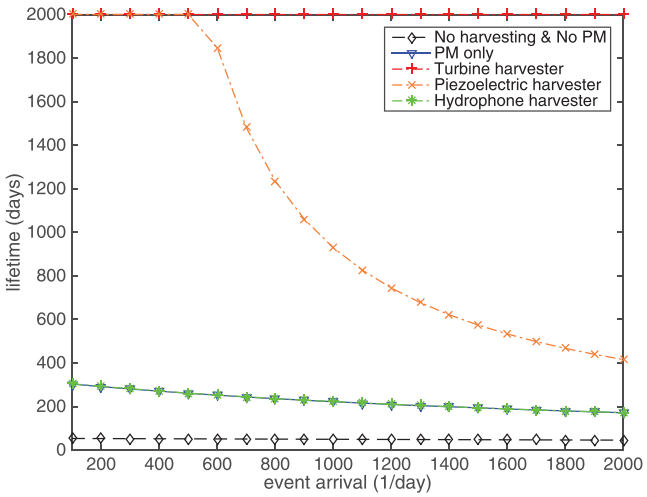

FIGURE 14 Lifetime improvement with event-driven operation at 400 m transmission range

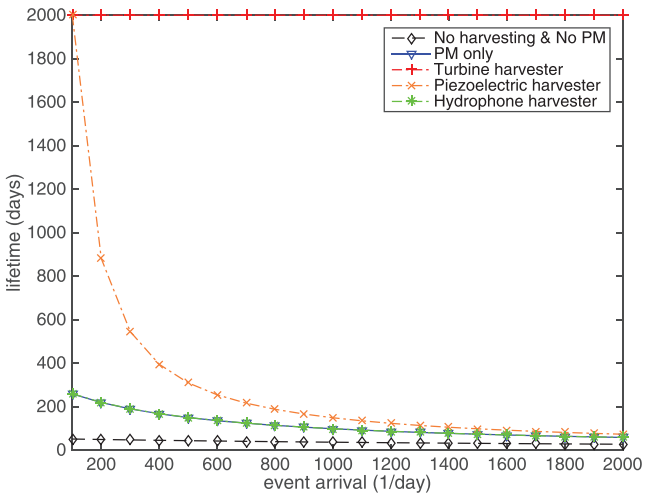

FIGURE 15 Lifetime improvement with event-driven operation at 800 m transmission range

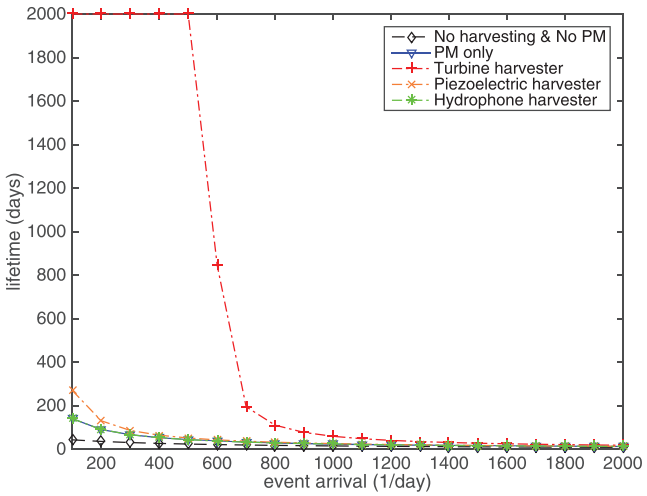

FIGURE 16 Lifetime improvement with event-driven operation at 1600 m transmission range

are depicted. Wherever the harvested power enables perpetual operation (ie, harvested power is bigger than consumed power) lifetime values are capped at 2000 days to conserve the details of results with low lifetime values.

Having the biggest harvested power output enables turbine harvester to provide perpetual lifetime for almost all duty cycle and event arrival values at all transmission ranges shorter than 1600 m (Figures 9, 10, 11, 13, 14, and 15). Figures 12 and 16 show that, at 1600 m of transmission range, the case is still valid until 0.3 duty cycle or 500 event arrivals. But, beyond these values, lifetime improvement almost vanishes no matter what harvester or power management scheme is used due to higher number of event detection and communication costs. As a result, turbine harvester should be preferred for applications without extreme conditions in similar environments. In extreme conditions, the benefit may not justify the increased cost.

The impact of piezoelectric harvester highly depends on the application scenario. Piezoelectric harvester is capable to provide perpetual lifetime for transmission ranges of 200 m and 400 m for low duty cycle or event arrival values as shown in Figures 9, 13, and 14. While schedule-driven operation at 200 m transmission range enables perpetual operation up to 0.15 duty cycle (Figure 9), event-driven operation enables it up to 1200 and 500 event arrivals at 200 m and 400 m transmission ranges, respectively (Figures 13 and 14). Therefore, piezoelectric harvester can be used in applications without strict missed event requirements.

The impact of hydrophone harvester cannot go beyond 2% of improvement under any scenario. This shows that the proposed harvesting technique is not yet viable even in a strait with high ship passages. However, a wider array of hydrophones or a closer positioning to passing ships may help improve the result. Also, as the technology develops, received voltage sensitivity of hydrophones may be improved in the future. Although preamplifiers are used for exactly this purpose, they are not utilized in this study since they are active devices and consume power to operate. Consequently, the usage of hydrophones as a medium for energy generation is not yet viable.

To compare the performances of event-driven and schedule-driven schemes, event-driven results at 1000 events/day can be used since this is the value that is also used in schedule-driven scheme. At this event arrival rate and 1600 m of transmission range, trigger-driven scheme provides 59 days of lifetime with turbine harvester (Figure 16). For schedule-driven scheme to provide at least the same lifetime, the duty cycle value should be decreased to 0.55 (Figure 12), which will cause high number of missed events.

At 800 m, both power management schemes enable perpetual operation with turbine harvester. Thus, piezoelectric harvester can be used for comparison. With event-driven scheme, the provided lifetime is at 149 days, while schedule-driven scheme requires duty cycle to be decreased to 0.3 to provide the same lifetime (Figures 11 and 15).

At 400 m, the lifetime event-driven scheme provides is 929 days. 0.15 is the maximum duty cycle for schedule-driven scheme that enables at least the same performance (Figures 10 and 14).

At 200 m, piezoelectric harvester enables perpetual operation; hence, hydrophone harvester can be used for comparison. With hydrophone harvester, lifetime with event-driven scheme is 266 days. For schedule-driven scheme to perform at least the same, the duty cycle value should be decreased to 0.1 (Figures 9 and 13).

Therefore, if the duty cycle values listed above meet the application requirements in terms of event miss probability, then schedule-driven scheme should be preferred. Otherwise, event-driven scheme outperforms schedule-driven scheme in exchange for higher costs due to additional hardware requirements.

5 | CONCLUSIONS AND FUTURE WORK

In this paper, different power management schemes and energy harvesters are examined with an objective of underwater node lifetime improvement. To this end, three different harvesting methods that exploit water flow and acoustic waves have been utilized. Specifically, the ambient energy present in water flow and acoustic waves are converted to electrical energy using hydrokinetic turbine, piezoelectric cantilever, and hydrophone to assist powering the nodes. Although hydrophones are usually utilized for monitoring tasks, their capability of converting acoustic waves into electrical signals enables them to be used as harvesters. In this scenario, the underwater streams and the acoustic noise generated by the ships passing through Istanbul Bosporus Strait is considered as the energy resource. Moreover, schedule-driven and event-driven power management schemes are utilized to extend node lifetime. Performance evaluations show that water flow–based energy harvesting methods can improve node lifetime substantially for different transmission distances considering real-life conditions of Istanbul Bosporus Strait. However, the impact of hydrophone harvester is negligible. Moreover, it is shown that event-driven management provides longer lifetime except extremely low duty cycle values. Consequently, this scheme should be preferred in applications intolerant to high sleep rates.

For further lifetime analysis, future work with a focus on a network with high number of nodes instead of a single node is planned. This way, the impact of routing on lifetime can be included in the analysis. Also, the impact of different MAC mechanisms is planned to be analyzed to show how variable delay characteristics of underwater environments affect the performance of MAC layer.

ACKNOWLEDGEMENT

This work was supported by the Turkish Scientific and Technical Research Council (TUBITAK) 1001 program under grant no. 114E248.

ORCID

H. Emre Erdem https://orcid.org/0000-0003-0127-2887
V. Cagri Gungor https://orcid.org/0000-0003-0803-8372

REFERENCES

1. Jawhar I, Mohamed N, Al-Jaroodi J, Zhang S. An efficient framework for autonomous underwater vehicle extended sensor networks for pipeline monitoring. *ROSE 2013-2013 IEEE Int Symp Robot Sensors Environ Proc*. 2013;124-129. https://doi.org/10.1109/ROSE.2013.6698430
2. Waldmeyer M, Tan HP, Seah WKG. Multi-stage AUV-aided localization for underwater wireless sensor networks. *Proceedings - 25th IEEE International Conference on Advanced Information Networking and Applications Workshops, WAINA*. 2011;2011:908-913. https://doi.org/10.1109/WAINA.2011.90
3. Akyildiz IF, Pompili D, Melodia T. Underwater acoustic sensor networks: research challenges. *Ad Hoc Networks*. 2005;3(3):257-279. https://doi.org/10.1016/j.adhoc.2005.01.004
4. Cui JH, Kong J, Gerla M, Zhou S. The challenges of building scalable mobile underwater wireless sensor networks for aquatic applications. *IEEE Netw*. 2006;20(3):12-18. https://doi.org/10.1109/MNET.2006.1637927
5. Basagni S, Di Valerio V, Gjanci P, Petrioli C. Harnessing HyDRO: Harvesting-aware Data ROuting for Underwater Wireless Sensor Networks. In: *Proceedings of the Eighteenth ACM International Symposium on Mobile Ad Hoc Networking and Computing - Mobihoc '18*. New York, New York, USA: ACM Press; 2018:271-279. https://doi.org/10.1145/3209582.3209610
6. Tandon S, Divi S, Muglia M, Vermillion C, Mazzoleni A. Modeling and dynamic analysis of a mobile underwater turbine system for harvesting marine hydrokinetic energy. *Ocean Eng*. 2019;187:106069. https://doi.org/10.1016/j.oceaneng.2019.05.051
7. Cario G, Casavola A, Lupia PGM, Petrioli C, Spaccini D. Long lasting underwater wireless sensors network for water quality monitoring in fish farms. In: *OCEANS* 2017 - Aberdeen. *IEEE*; 2017:1-6. https://doi.org/10.1109/OCEANSE.2017.8084777
8. Michelin S, Doaré O. Energy harvesting efficiency of piezoelectric flags in axial flows. *J Fluid Mech*. 2013;714:489-504. https://doi.org/10.1017/jfm.2012.494
9. Molino-Minero-Re E, Carbonell-Ventura M, Fisac-Fuentes C, Manuel-Lazaro A, Toma DM, Piezoelectric energy harvesting from induced vortex in water flow. IEEE international instrumentation and measurement technology conference proceedings. *IEEE*. 2012;2012:624-627. https://doi.org/10.1109/I2MTC.2012.6229686
10. Shahab S, Erturk A. Electrohydroelastic Dynamics of Macro-Fiber Composites for Underwater Energy Harvesting from Base Excitation. 2014;9057:90570C. https://doi.org/10.1117/12.2045180
11. Toma DM, del Rio J, Carbonell-Ventura M, Masalles JM. Underwater energy harvesting system based on plucked-driven piezoelectrics. In: *OCEANS* 2015 - Genova. *IEEE*; 2015:1-5. https://doi.org/10.1109/OCEANS-Genova.2015.7271599
12. Li H, Tian C, Lu J, et al. An energy harvesting underwater acoustic transmitter for aquatic animals. *Sci Rep*. 2016;6(1):33804. https://doi.org/10.1038/srep33804
13. Cha Y, Abdolhamidi S, Porfiri M. Energy harvesting from underwater vibration of an annular ionic polymer metal composite. *Meccanica*. 2015;50(11):2675-2690. https://doi.org/10.1007/s11012-015-0165-5
14. Rezaei HF, Kruger A, Just C, An energy harvesting scheme for underwater sensor applications. IEEE international conference on electro/information technology. *IEEE*. 2012;2012:1-4. https://doi.org/10.1109/EIT.2012.6220721
15. Wang L, Lei Y, Li B, Cui J-H. Towards achieving long-lifespan and self-sustained monitoring of coastal environments. In: 2014 *IEEE International Conference on Systems, Man, and Cybernetics (SMC)*. Vol 2014-Janua. IEEE; 2014:3413-3418. https://doi.org/10.1109/SMC.2014.6974456
16. Mayer P, Magno M, Benini L. Self-sustaining acoustic sensor with programmable pattern recognition for underwater monitoring. *IEEE Trans Instrum Meas*. 2019;68(7):2346-2355. https://doi.org/10.1109/TIM.2018.2890187

17. Bereketli A, Bilgen S. Remotely powered underwater acoustic sensor networks. *IEEE Sens J*. 2012;12(12):3467-3472. https://doi.org/10.1109/JSEN.2012.2210401
18. Erdem HE, Gungor VC. Lifetime analysis of energy harvesting underwater wireless sensor nodes. In: *Signal Processing and Communications Applications Conference (SIU),* 2017 25th. IEEE; 2017:1-4.
19. Erturk A, Delporte G. Underwater thrust and power generation using flexible piezoelectric composites: an experimental investigation toward self-powered swimmer-sensor platforms. *Smart Mater Struct*. 2011;20(12):125013. https://doi.org/10.1088/0964-1726/20/12/125013
20. Zhu G, Su Y, Bai P, et al. Harvesting water wave energy by asymmetric screening of electrostatic charges on a nanostructured hydrophobic thin-film surface. *ACS Nano*. 2014;8(6):6031-6037. https://doi.org/10.1021/nn5012732
21. Jarosz E, Teague WJ, Book JW, Beşiktepe Ş. On flow variability in the Bosphorus Strait. *J Geophys Res*. 2011;116(C8):C08038. https://doi.org/10.1029/2010JC006861
22. Vermaak HJ, Kusakana K, Koko SP. Status of micro-hydrokinetic river technology in rural applications: a review of literature. *Renew Sustain Energy Rev*. 2014;29:625-633. https://doi.org/10.1016/j.rser.2013.08.066
23. Hoq T, Nawshad UA, Islam N, Syfullah K, Rahman R. Micro hydro power: promising solution for off-grid renewable energy source. *Int J Sci Eng Res*. 2011;2(12):2-6.
24. Pobering S, Ebermeyer S, Schwesinger N. Generation of electrical energy using short piezoelectric cantilevers in flowing media S. 2009;7288:728807-728807-728807-728808. https://doi.org/10.1117/12.815189
25. Pobering S, Schwesinger N. A novel hydropower harvesting device. *MEMS, NANO Smart Syst 2004 ICMENS 2004 Proceedings 2004 Int Conf*. 2004;2004:480-485. https://doi.org/10.1109/ICMENS.2004.1508997
26. HTI-90-U Hydrophone. http://www.hightechincusa.com/products/hydrophones/hti90u.html.
27. McKenna MF, Ross D, Wiggins SM, Hildebrand JA. Underwater radiated noise from modern commercial ships. *J Acoust Soc am*. 2012;131(1):92-103. https://doi.org/10.1121/1.3664100
28. Jung D, Teixeira T, Savvides A. Sensor node lifetime analysis: models and tools. *ACM Trans Sens Networks*. 2009;5(1):1-33. https://doi.org/10.1145/1464420.1464423
29. Directional Hydrophone (Acoustic Sensor). http://www.benthowave.com/products/BII-7070Hydrophone.html.
30. PIC10F200-8-bit PIC Microcontrollers. http://www.microchip.com/wwwproducts/en/en019863.
31. Lanbo L, Shengli Z, Jun-Hong C. Prospects and problems of wireless communication for underwater sensor networks. *Wirel Commun Mob Comput*. 2008;8(8):977-994. https://doi.org/10.1002/wcm.654
32. Felemban M, Felemban E. Energy-delay tradeoffs for underwater acoustic sensor networks. *First Int Black Sea Conf Commun Netw*. 2013;2013:45-49. https://doi.org/10.1109/BlackSeaCom.2013.6623379
33. Evologics GmbH. Products _ Underwater Acoustic Modems _ S2CR 48_78 Acoustic Modem _ EvoLogics GmbH. https://www.evologics.de/en/products/acoustics/s2cr_48_78.html. .
34. Lin JH, Wu XM, Ren TL, Liu LT. Modeling and simulation of piezoelectric MEMS energy harvesting device. *Integr Ferroelectr*. 2007;95(1):128-141. https://doi.org/10.1080/10584580701756649
35. Li B, You JH. Simulation of acoustic energy harvesting using piezoelectric plates in a quarter-wavelength straight-tube resonator. *Proc 2012 COMSOL Conf Bost*. 2012.
36. Gao X, Shih W-H, Shih WY. Flow energy harvesting using piezoelectric cantilevers with cylindrical extension. *Ind Electron IEEE Trans*. 2013;60(3):1116-1118. https://doi.org/10.1109/TIE.2012.2187413

How to cite this article: Erdem HE, Gungor VC. Analyzing lifetime of energy harvesting underwater wireless sensor nodes. *Int J Commun Syst*. 2020;33:e4214. https://doi.org/10.1002/dac.4214